Investigation of the hyperfine structure of Ta I lines (X)

2006 Phys. Scr. 74 211

(http://iopscience.iop.org/1402-4896/74/2/011)

Phys. Scr. **74** (2006) 211–217 doi:10.1088/0031-8949/74/2/011

Investigation of the hyperfine structure of Ta I lines (X)

N Jaritz[1], L Windholz[1], U Zaheer[1], M Farooq[1], B Arcimowicz[2], R Engleman Jr[3], J C Pickering[4], H Jäger[1] and G H Guthöhrlein[5]

[1] Institut für Experimentalphysik, Technische Universität Graz, Petersgasse 16, A-8010 Graz, Austria
[2] Institute of Physics, Poznań Technical University, Pl-60–965 Poznań, Poland
[3] Department of Chemistry, University of New Mexico, Albuquerque, NM 87131, USA
[4] Blackett Laboratory, Imperial College London, Prince Consort Road, London, UK
[5] Laboratorium für Experimentalphysik, Universität der Bundeswehr Hamburg, Holstenhofweg 85, D-22043 Hamburg, Germany

E-mail: windholz@tugraz.at

Received 27 October 2005
Accepted for publication 10 April 2006
Published 18 July 2006
Online at stacks.iop.org/PhysScr/74/211

Abstract
We report the discovery of 23 new energy levels of even parity and 21 new energy levels of odd parity of the tantalum atom. The results given here are based on investigations of the hyperfine structure of 221 new spectral lines of the tantalum atom (Ta I) by means of laser spectroscopic methods, detecting laser-induced fluorescence. The excitation wavelengths were extracted from high-resolution Fourier transform spectra.

PACS number: 31.10.Fn

1. Introduction

The electronic shell of the tantalum isotope ^{181}Ta has been investigated by our group since 1990 [1–9]. In the first few papers [1–5], the main point was the determination of the hyperfine (hf) constants of already known levels, while later [5–9] the finding of up to the time of publication unknown energy levels was the main purpose of the investigations. At the beginning of the investigations, only photographic spectra produced by B Arcimowicz using a grating spectrograph with a 2 m focal length in fifth order were available. In recent years, additional spectra, acquired by J C Pickering and R Engleman using the technique of Fourier transform (FT) spectroscopy, were analysed.

A huge number of additional lines, not listed in commonly used spectral tables, were found in these spectra [10–12]. As the nuclear momentum of tantalum is $I = 7/2$, all lines show hf structures due to characteristic properties of the levels involved. In most cases these lines could be classified as transitions between known Ta levels, from their wavenumber and their observed hf pattern resolved in the FT spectra. Other lines, however, required investigations using laser excitation methods, particularly when the centre of gravity wavenumbers of the lines did not match energy differences between known levels, and/or when the observed hyperfine patterns did not match patterns predicted assuming transitions between known energy levels. In these cases the method of laser-induced-fluorescence (LIF) spectroscopy was used. From the recorded hf pattern, the angular momenta J, the magnetic dipole constants A and the electric quadrupole constants B of the levels involved were determined. These characteristic properties, together with the centre of gravity wavenumbers of the excited and of the fluorescence lines, led to the determination of the energy of the new level. In most cases the newly introduced level could be confirmed by at least one further excitation.

Additionally, some previously unknown levels were found by analysing the FT spectra (for methods, see [13]). The existence of these levels was often confirmed later by laser excitation.

2. Experimental details

The experimental setup was the same as used previously for the work on Ta I. A sketch of the arrangement is given in [5]. By cathode sputtering, free tantalum atoms were produced in a hollow cathode lamp with an inner diameter of 3 mm and a cathode length of 15–20 mm. The cathode current was typically 60 mA. Argon was used as the discharge gas, with a pressure between 1 and 1.5 mbar. The emission spectrum of the Ta–Ar plasma contains mainly Ta I lines, but also lines of Ta II.

0031-8949/06/020211+07$30.00

Table 1. Ta I lines investigated by laser excitation.

λ/Å	SNR	*J*-values Even	*J*-values Odd	Level energies (cm^{-1}) Even	Level energies (cm^{-1}) Odd
4236.060	nl < 1	7/2	5/2	29276.388	52876.59[a]
4241.872	nl < 1	13/2	11/2	30542.35	54110.21[a]
4245.087	nl2	9/2	9/2	55080.053[a]	31530.050
4245.850	nl5	5/2	5/2	41539.61	17993.726
4246.599	nl < 1	3/2	5/2	52885.13[a]	29343.501
4256.509	nl < 1	11/2	9/2	52253.46[a]	28766.644
4309.504	nl < 1	3/2	3/2	54751.88[a]	31553.879
4325.930	nl10	5/2	3/2	53774.61[a]	30664.684
4326.020	nl < 1	5/2	5/2	48290.642	25181.186
4327.192	nl < 1	7/2	5/2	25894.22	48997.39[a]
4334.720	nl < 1	9/2	9/2	54593.11[a]	31530.050
4346.466	nl < 1	7/2	9/2	22761.279	45762.010
4356.529	nl < 1	9/2	7/2	55080.053[a]	32132.453
4369.423	nl < 1	5/2	3/2	53774.61[a]	30894.719
4382.645	nl < 1	5/2	5/2	23512.447	46323.311
4388.558	nl < 1	11/2	11/2	33064.153	55844.28[a]
4393.990	nl2	7/2	7/2	50532.56	27780.652
4399.403	nl2	3/2	1/2	49590.12[a]	26866.045
4402.630	nl7	7/2	7/2	24917.996	47625.030
4414.249	nl3	1/2	1/2	49513.59[a]	26866.045
4415.540	nl < 1	7/2	5/2	49435.71	26794.812
4451.110	nl3	1/2	1/2	20144.81	42604.76[a]
4455.308	nl2	9/2	11/2	32192.70	54631.54[a]
4544.163	nl4	5/2	7/2	46981.974	24981.880
5596.932	nl2	5/2	3/2	24546.202	42408.185
5600.105	nl5	7/2	9/2	53349.80	35497.669
5613.680	nl4	9/2	11/2	25376.469	43185.120
5675.823	nl4	7/2	5/2	46958.11	29343.501
5683.858	nl5	7/2	9/2	51204.28	33615.515
5747.650	nl 3	5/2	5/2	27715.82	45109.373
5752.535	nl3	1/2	3/2	20144.81	37523.584
5755.022	nl 2	5/2	3/2	21623.018	38994.377
5778.559	nl 3	7/2	5/2	53314.62[a]	36014.068
5779.195	nl < 1	1/2	3/2	49513.59[a]	32214.941
5799.810	nl < 1	9/2	11/2	53050.68[a]	35813.517
5827.477	nl < 1	7/2	7/2	53314.62[a]	36159.292
5838.923	nl 3	3/2	5/2	54751.88[a]	37630.196
5840.850	nl < 1	7/2	7/2	54677.34[a]	37561.288
5841.084	nl 5	3/2	5/2	33676.410	50791.77[a]
5855.100	nl 2	13/2	13/2	56435.09[a]	39360.710
5889.165	nl 4	7/2	5/2	26575.220	43550.795
5889.908	nl 8	5/2	3/2	27715.82	44689.309
5891.893	nl < 1	7/2	9/2	53598.985[a]	36631.213
5899.911	nl 2	9/2	9/2	29116.264	46060.53
5914.160	nl < 1	5/2	7/2	51703.645	34799.731
5922.507	nl 20	7/2	7/2	22761.279	39641.344
5928.887	nl < 1	5/2	7/2	31719.773	48581.67[a]
5936.393	nl 9	7/2	5/2	29276.388	46116.938
5937.740	nl 8	9/2	11/2	49907.096	33070.364
5951.060	nl 5	7/2	7/2	53598.985[a]	36799.905
5963.803	nl 3	5/2	3/2	35065.694	51828.83[a]
5965.530	nl 7	1/2	3/2	22236.014	38994.377
5965.837	nl 3	5/2	3/2	31719.773	48477.26[a]
5970.130	nl 2	7/2	7/2	30879.724	47625.030
5992.991	nl 4	9/2	7/2	33978.88	50660.46[a]
6005.861	nl 4	9/2	9/2	29116.264	45762.010
6023.346	nl 15	9/2	11/2	23912.929	40510.392
6081.060	nl < 1	11/2	11/2	52253.46[a]	35813.517
6098.260	nl 4	11/2	9/2	53024.61	36631.213
6099.977	nl 3	9/2	7/2	32192.70	48581.67[a]
6101.198	nl 6	5/2	5/2	50386.89	34001.203
6106.328	nl < 1	7/2	7/2	29276.388	45648.307
6106.344	nl < 1	3/2	3/2	55959.631	39587.753
6114.299	nl < 1	3/2	5/2	32187.394	48537.973

Table 1. Continued.

λ/Å	SNR	*J*-values Even	*J*-values Odd	Level energies (cm^{-1}) Even	Level energies (cm^{-1}) Odd
6115.370	nl 5	5/2	5/2	43142.50	26794.812
6122.864	nl 10	5/2	5/2	44461.647	28133.941
6125.391	nl 4	1/2	3/2	48535.93	32214.941
6125.958	nl 8	3/2	1/2	32187.394	48506.91[a]
6129.092	nl 6	3/2	3/2	15903.818	32214.941
6131.380	nl < 1	3/2	5/2	33676.410	49981.439
6131.900	nl 3	9/2	7/2	51103.31	34799.731
6137.095	nl 5	3/2	3/2	32187.394	48477.26[a]
6141.713	nl < 1	5/2	7/2	35065.694	51343.29[a]
6143.923	nl < 1	7/2	5/2	52285.81	36014.068
6143.990	nl 8	1/2	1/2	22236.014	38507.611
6150.283	nl 4	7/2	5/2	34536.885	50791.77[a]
6152.470[b]	nl 8	3/2	5/2	21381.052	37630.196
6157.316	nl 5	5/2	5/2	34514.897	50751.28[a]
6157.999	nl 10	3/2	5/2	24275.959	40510.392
6159.754	nl < 1	3/2	3/2	47124.64	30894.719
6160.009	nl 15	5/2	3/2	44918.665	28689.339
6162.090	nl < 1	5/2	5/2	25655.493	41879.253
6163.070	nl 3	7/2	9/2	9705.350	25926.383
6163.210	nl < 1	7/2	7/2	35122.47	51343.29[a]
6165.628	nl 10	7/2	5/2	34536.885	50751.28[a]
6167.978	nl 10	5/2	5/2	31719.773	47928.08
6179.379	nl 5	3/2	5/2	52054.91	35876.551
6180.065	nl < 1	7/2	7/2	26575.220	42751.800
6181.431	nl < 1	9/2	9/2	54115.93	37942.923
6184.489	nl 4	5/2	5/2	27715.82	43880.820
6185.545	nl 4	11/2	11/2	55630.89	39468.660
6191.938	nl < 1	5/2	7/2	34514.897	50660.46[a]
6194.438	nl 8	9/2	9/2	15391.019	31530.050
6194.710	nl 3	3/2	5/2	27412.44	43550.795
6200.391	nl 8	7/2	7/2	34536.885	50660.46
6204.090	nl 2	7/2	9/2	17383.173	33497.154
6216.334	nl 4	3/2	1/2	41594.852	25512.659
6227.396	nl < 1	7/2	5/2	30879.724	46933.359
6264.941	nl 6	5/2	7/2	51703.645	35746.232
6285.491	nl < 1	5/2	7/2	31719.773	47625.030
6286.145	nl < 1	9/2	7/2	33978.88	49882.486
6303.113	nl 8	1/2	1/2	26743.950	42604.76[a]
6313.388	nl < 1	5/2	5/2	27715.82	43550.795
6316.025	nl < 1	7/2	7/2	34536.885	50365.26
6319.070	nl 5	3/2	1/2	49381.988	33561.282
6330.113	nl 8	5/2	3/2	24546.202	40339.329
6336.728	nl < 1	3/2	1/2	34969.95	50746.60[a]
6353.820	nl 6	3/2	3/2	51455.10[a]	35720.898
6364.966[c]	nl 10	7/2	9/2	51204.28	35497.669
6365.688	nl 5	3/2	5/2	25876.05	41580.975
6366.308	nl 1	9/2	11/2	33978.88	49682.230
6368.066	nl 8	13/2	13/2	55059.72[a]	39360.710
6371.359	nl 13	9/2	9/2	29116.264	44806.789
6372.540	nl 6	7/2	5/2	48872.99	33185.006
6387.420	nl 2	9/2	11/2	53845.74	38194.285
6388.930	nl 2	9/2	7/2	51394.01	35746.232
6396.283	nl < 1	3/2	1/2	34969.95	50599.71[a]
6399.874	nl 8	5/2	5/2	32916.837	48537.973
6411.587	nl 6	7/2	5/2	24917.996	40510.392
6412.160	nl < 1	13/2	11/2	55059.72[a]	39468.660
6413.764	nl < 1	5/2	7/2	50386.89	34799.731
6414.428	nl < 1	5/2	7/2	51331.776	35746.232
6417.320	nl 6	3/2	5/2	51455.10[a]	35876.551
6424.861	nl 4	5/2	3/2	32916.837	48477.26[a]
6431.721	nl 8	5/2	3/2	49622.187	34078.456
6440.266	nl < 1	9/2	7/2	50322.852[a]	34799.731
6442.354	nl < 1	5/2	3/2	50760.94[a]	35242.955
6444.979	nl < 1	3/2	3/2	49590.12[a]	34078.456

Table 1. Continued.

		J-values		Level energies (cm^{-1})	
λ/Å	SNR	Even	Odd	Even	Odd
6450.354	nl < 1	3/2	3/2	54751.88[a]	39253.139
6457.361	nl 10	5/2	3/2	23512.447	38994.377
6464.796	nl 5	5/2	7/2	51210.36[a]	35746.232
6467.056	nl 8	3/2	3/2	47012.63	31553.879
6469.696	nl 5	5/2	5/2	32916.837	48369.457
6476.937	nl 2	1/2	3/2	49513.59[a]	34078.456
6478.112	nl < 1	9/2	7/2	32192.70	47625.030
6479.892[d]	nl < 1	5/2	3/2	46981.974	31553.879
6496.887	nl 2	9/2	7/2	55323.98[a]	39936.246
6498.630	nl 4	5/2	3/2	34514.897	49898.50[a]
6499.731	nl 3	5/2	7/2	46981.974	31600.982
6507.867	nl 3	5/2	7/2	43142.50	27780.652
6509.832	nl 3	7/2	7/2	46958.11	31600.982
6513.385	nl 5	5/2	3/2	32916.837	48265.6[a]
6524.920	nl 2	3/2	3/2	25876.05	41197.664
6526.304	nl < 1	9/2	11/2	53512.66[a]	38194.285
6530.675	nl 4	11/2	9/2	29498.604	44806.789
6532.410	nl 8	7/2	5/2	26575.220	41879.253
6532.600	nl 5	3/2	3/2	49381.988	34078.456
6534.327	nl < 1	5/2	7/2	35065.694	50365.26
6535.650	nl 3	13/2	11/2	30542.35	45838.890
6537.675	nl < 1	9/2	9/2	50509.674	35217.944
6539.466	nl 10	1/2	3/2	22236.014	37523.584
6539.990	nl 4	9/2	7/2	29116.264	44402.618
6544.577	nl 8	9/2	11/2	45636.874	30361.262
6557.167	nl < 1	7/2	7/2	50992.506	35746.232
6560.712	nl < 1	11/2	13/2	54598.745	39360.710
6565.992	nl 4	1/2	1/2	22236.014	37461.485
6570.861	nl 4	7/2	5/2	3963.922	19178.426
6571.257	nl < 1	5/2	5/2	31719.773	46933.359
6574.385	nl 3	5/2	7/2	53459.935	38253.433
6575.875	nl 8	5/2	5/2	21623.018	36825.980
6580.455	nl 10	3/2	1/2	27412.44	42604.76[a]
6585.446	nl < 1	7/2	9/2	30879.724	46060.53
6598.112	nl < 1	7/2	7/2	49246.36	34094.692
6603.562	nl < 1	5/2	3/2	36689.667	51828.83[a]
6609.217	nl 3	7/2	7/2	29276.388	44402.618
6610.790	nl 4	5/2	7/2	32502.382	47625.030
6615.007	nl < 1	11/2	9/2	53055.89[a]	37942.923
6620.051	nl < 1	9/2	11/2	53295.74	38194.285
6620.895	nl < 1	7/2	7/2	20646.702	35746.232
6635.249	nl 10	7/2	9/2	26575.220	41641.967
6635.520	nl 2	7/2	9/2	26575.220	41641.967
6636.134	nl < 1	7/2	5/2	49857.127	34792.275
6638.406	nl < 1	3/2	1/2	48620.98	33561.282
6650.469	nl 5	9/2	9/2	53845.74	38813.342
6669.730	nl 3	9/2	9/2	58079.070	43090.337
6680.450	nl 4	3/2	1/2	21381.052	36345.871
6680.530	nl 6	3/2	1/2	21381.052	36345.871
6680.870	nl 2	5/2	5/2	43825.98	28862.036
6682.757	nl 4	5/2	7/2	43142.50	28182.633

Table 1. Continued.

		J-values		Level energies (cm^{-1})	
λ/Å	SNR	Even	Odd	Even	Odd
6684.400	nl 2	9/2	7/2	25376.469	40333.027
6691.494	nl 5	5/2	3/2	26752.40	41692.621
6697.152	nl < 1	1/2	3/2	29761.71	44689.309
6713.000	nl 2	7/2	9/2	35122.47	50014.147
6713.715	nl 4	7/2	5/2	54677.34[a]	39786.599
6714.426	nl 5	7/2	7/2	29276.388	44165.583
6716.813	nl < 1	9/2	7/2	51683.81	36799.905
6717.542	nl < 1	7/2	9/2	30879.724	45762.010
6739.172	nl 4	5/2	3/2	36689.667	21855.124
6739.950	nl 4	5/2	3/2	35065.694	49898.50[a]
6744.658	nl < 1	5/2	7/2	49622.187	34799.731
6760.525	nl 6	1/2	3/2	41151.381	26363.721
6763.641	nl 4	5/2	7/2	53459.935	38679.181
6764.524	nl 4	3/2	5/2	46740.349	31961.442
6769.260	nl < 1	7/2	7/2	30879.724	45648.307
6771.618	nl < 1	9/2	7/2	50509.674	35746.232
6790.253	nl 3	1/2	3/2	6049.433	20772.357
6791.150	nl 6	5/2	7/2	42501.635	27780.652
6792.323	nl 5	3/2	3/2	24275.959	38994.377
6793.573	nl 8	7/2	9/2	46245.79	31530.050
6798.016	nl 1	5/2	5/2	53459.935	38753.816
6808.320	nl 10	5/2	3/2	25655.363	40339.329
6809.770	nl 10	3/2	3/2	22842.851	37523.584
6830.830	nl 4	7/2	7/2	53314.62[a]	38679.181
6831.357	nl 4	3/2	5/2	25876.05	40510.392
6836.647	nl 3	5/2	7/2	53302.234	38679.181
6838.162	nl < 1	3/2	5/2	48620.98	34001.203
6838.797	nl 6	3/2	1/2	22842.851	37461.485
6852.788	nl 1	1/2	3/2	29761.71	44350.284
6857.630	nl 6	7/2	5/2	17383.173	31961.442
6858.458	nl 4	9/2	7/2	50322.75[a]	35746.232
6874.488	nl < 1	3/2	3/2	48620.98	34078.456
6887.490	nl 4	13/2	11/2	30542.35	45057.494
6919.377	nl 6	5/2	3/2	24546.202	38994.377
6919.786	nl 4	13/2	11/2	54957.71	40510.392
6922.256	nl 5	1/2	1/2	49513.59[a]	35071.362
6945.624	nl 5	9/2	9/2	55080.053[a]	40686.463
6964.800	nl 3	3/2	3/2	25876.05	40230.036
6981.802[e]	5	5/2	7/2	42501.635	28182.633
7003.609	nl 7	7/2	5/2	29276.388	43550.795
7008.296	nl 10	9/2	7/2	25376.469	39641.344
7012.252	nl 7	7/2	7/2	29276.388	43533.214

[a] New level, see table 2.
[b] Blend situation with 6152.511→, 43 982.532-27 733.511 cm^{-1} (classified in [12]).
[c] Blend situation with 6364.902→, 42 501.635-26 794.812 cm^{-1} (classified in [18]).
[d] Blend situation with 6479.908→, 46 958.11-31 530.050 cm^{-1} (classified in [6]).
[e] Wavelength in [17] 6981.990→.

The advantage of this method is that it not only produces tantalum atoms in the ground state, but also in higher excited states with a population large enough to enable laser excitation. To reduce the Doppler width of the hf components the hollow cathode lamp was cooled by liquid nitrogen.

The tantalum–argon plasma within the hollow cathode lamp was irradiated by laser light generated by a tuneable cw dye laser, whose intensity had been modulated by a chopper wheel. The fluorescence lines were selected by a grating monochromator and detected by a photomultiplier. The laser-induced change of the fluorescence signal was intensified by a lock-in amplifier with the frequency of the chopper wheel as reference. The hf structure was recorded digitally for further evaluation.

For transitions, which were not classified before, the frequency of the laser was set on the strongest hf component of the spectral line under investigation, and LIF signals were searched by scanning a grating monochromator. If at least one LIF signal was found, the laser frequency was scanned over the entire spectral line and its hf pattern was recorded using the fluorescence line with the best signal to noise ratio.

Since the reading precision of the monochromator used was about ±1 Å, it was sometimes necessary to determine the

Table 2. Energy values, J-values, hf interaction constants and excitation wavelength(s) of the new Ta I levels.

Energy (cm^{-1})	J	A (MHz)	B (MHz)	λ_{exc} (Å)	Comment
Even parity					
49 513.59(5)	1/2	−1458(25)	0	(3348.471), 4414.249, 5779.195, 6476.937, 6922.256	
49 590.12(2)	3/2	−125(10)	−360(150)	(3104.165), 4399.403, 6444.979	A and B by fitting 3104.165, 3287.265, 3810.665, 3944.180 from FT spectra
50 322.75(1)	9/2	673.8(30)	−1025(50)	6440.266, 6858.458	
50 760.94(4)	5/2	616(30)	−290(200)	(3050.943), 6442.354	A and B by fitting 3050.943, 3458.521, 3481.668 from FT spectra
51 119.81(5)	3/2	2041(45)	−281(400)	(3337.691)	A and B by fitting 3337.691, 3438.710, 4109.851 from FT spectra[a]
51 210.36(4)	5/2	598(4)	115(130)	(3589.994), 6464.796	
51 455.10(3)	3/2	776(4)	−275(30)	6353.820, 6417.320	
52 253.46(2)	11/2	953(2)	−907(100)	(3669.412), 4256.509, 6081.060	
52 885.13(1)	3/2	411(6)	−70(200)	(3385.446), 4246.599	A and B by fitting 2907.785, 3652.264, 3385.446 from FT spectra
53 050.68(3)	9/2	977.8(9)	−354(70)	(3432.614), 5799.810	
53 055.89(3)	11/2	449.7(5)	370(180)	(3291.320), 6615.007	A and B by fitting 3291.320, 4115.891, 5142.500 from FT spectra
53 314.62(3)	7/2	203(10)	−460(70)	5778.559, 5827.477, 6830.830	
53 512.66(2)	9/2	1009(3)	−802(220)	(3242.557), 6526.304	
53 598.985(10)	7/2	390(4)	518(35)	5891.893, 5951.060	
53 774.61(2)	5/2	412(5)	−723(180)	4325.930, 4369.423	
54 593.11(3)	9/2	432(10)	1200(400)	(3103.473), 4334.720	
54 677.34(3)	7/2	917.3(2)	1184(40)	5840.850, 6713.715	
54 751.88(3)	3/2	632(15)	111(60)	4309.504, 5838.923, 6450.354	
55 059.72(1)	13/2	1030(3)	700(100)	6368.066, 6412.160	
55 080.053(8)	9/2	881.3(20)	641(15)	4245.087, 4356.529, 6945.624	
55 323.98(3)	9/2	603(5)	413(220)	(3294.802), 6496.887	
56 435.09(1)	13/2	1041(5)	−300(400)	(3488.526), 5855.100	
Odd parity					
42 604.76(5)	1/2	1562(6)	0	6303.113, 6580.455	
48 265.60(1)	3/2	73.7(2)	300(12)	6513.385	
48 477.26(3)	3/2	753(1)	381(30)	5965.837, 6137.095, 6424.861	
48 506.91(5)	1/2	2879(6)	0	(14463.51), 6125.958	
48 581.67(3)	7/2	742.2(10)	1297(8)	5928.887, 6099.977	
48 997.39(2)	5/2	818(3)	110(100)	(3620.014), 4327.192	A and B by fitting 3620.014, 13 519.240, 15 390.410 from FT spectra
49 898.50(3)	3/2	1190(5)	606(60)	6498.630, 6739.950	
50 599.71(2)	1/2	−464.5(20)	0	(3282.596), 6396.283	
50 660.46(4)	7/2	700(6)	196(100)	5992.991, 6191.938, 6200.391	
50 746.60(5)	1/2	−1390(2)	0	(3266.837), 6336.728	
50 751.28(5)	5/2	866.3(10)	182(50)	6157.316, 6165.628	
50 791.77(3)	5/2	980.7(7)	58(9)	5841.084, 6150.283	
51 207.82(4)	7/2	592(5)	436(150)	(3271.189)	A and B by fitting 3271.189, 3379.148, 14 819.230 from FT spectra[a]
51 343.29(2)	7/2	456(6)	−225(25)	(3592.110), 6141.713, 6163.210	A and B by fitting 3256.753, 3497.705, 3592.110 from FT spectra
51 828.83(3)	3/2	335(5)	275(20)	(3378.229), 5963.803, 6603.562	
52 876.59(2)	5/2	456.3(10)	−380(90)	(3404.537), 4236.060	A and B by fitting 3404.537, 3328.631, 16 960.020 from FT spectra
54 110.21(1)	11/2	653(5)	71(150)	(3310.603), 4241.872	A and B by fitting 3155.046, 3267.535, 3310.603 from FT spectra
54 631.54(3)	11/2	671(8)	25(200)	(3254.416), 4455.308	A and B by fitting 3104.413, 3254.416, 3417.232 from FT spectra
54 831.96(1)	15/2	150.3(10)	3658(25)	(3192.227)	A and B by fitting only 3192.227 from FT spectra[a]
55 785.57(5)	9/2	370(3)	658(25)	(2997.005)	A and B by fitting 2997.005, 3238.710 from FT spectra[a]
55 844.28(3)	11/2	274(10)	1580(400)	(3130.811), 4388.558	

[a]Level not confirmed by excitation with laser light.

wavelengths of the LIF lines more accurately. This was done by using the second chopper wheel in front of the input slit of the monochromator to modulate the whole fluorescence light of the hollow cathode lamp. The output signal of the photomultiplier then also became the input for a second lock-in amplifier, with the frequency of the second chopper wheel as reference. The grating monochromator was then scanned over a certain spectral range, with the laser light frequency set to the highest component of the excited hf pattern, and the output signals of both lock-in amplifiers were recorded simultaneously on separate traces. In this way the spectrum of the hollow cathode lamp can be used to calibrate the monochromator wavelength scale. The recorded hollow cathode spectra were compared with the corresponding parts of the FT spectra. In this way, the wavelength of a LIF line could be determined with an accuracy of ~ 0.05 Å, despite the relatively low resolution of our monochromator (focal length 0.5 m).

The wavelength calibrated FT spectra (see [7]) cover a broad range of wavelengths from 2000 to 50 000 Å. Using the dispersion formula of Peck and Reeder [14] for the refractive index of the air, the centre-of-gravity air wavelengths of the Ta lines were determined. For weak lines, the uncertainty is less than ± 0.003 Å, mainly caused by the noise of the FT spectra [15]. The FT spectra contain completely or at least partially resolved hf patterns. Although the resolution is limited by the Doppler line widths of the hf components, the line profile often allows the identification of the transition, when the hf constants of the levels involved are known or can be determined. Due to the high wavelength accuracy of the FT spectra and the good accuracy of the lambdameter used, the wavelength of the laser light was precisely set to an hf component of the investigated line. A computer program [13] was used to propose suggestions for line classification. These possibilities were then either rejected or confirmed by selecting certain fluorescence lines by means of the monochromator to confirm the increase or diminution of the population density of one of the combining levels through the use of the laser. By looking at the possible classifications proposed by the computer program for the line under investigation, inappropriate possibilities could be excluded when the corresponding hf structure pattern was found not to fit the observed hf pattern, and blend situations were confirmed by laser excitation.

If at least one unknown energy level was involved in the excited transition, no useful suggestion for classification was available. With the laser light frequency fixed at the highest hf component observed in the FT spectrum, LIF signals were searched by scanning the monochromator. If at least one LIF signal was successfully found, the hf pattern was recorded by scanning the laser frequency over a certain range (up to 40 GHz).

3. Results and discussion

Table 1 lists all excited new lines. The wavelengths are given in Å (in air) in column 1. Column 2 contains the signal-to-noise ratio (SNR) of the lines observed in the FT spectra. Because the FT spectra are not intensity calibrated, the SNR provides only a very approximate idea of the line intensity. When a line from the list was excited, but did not appear in the FT spectra, the wavelength calculated from the level energies is given and the intensity was set to '<1'. The designation 'nl' means 'new line'. In columns 3 and 4, the J-values of the combining levels are listed, and their energy values are given in columns 5 and 6. A new energy level involved in the transition is distinguished by remark 'a' after the energy value of the level. As in our earlier papers [6–9], for previously known levels we have used improved energy values obtained by R Engleman [16] from the analysis of FT spectra, as far as available.

Table 3. Improved energy values for some Ta I energy levels of even parity.

J-value	Energy (cm^{-1}) this work	Energy (cm^{-1})	Earlier works
7/2	25 894.22(2)	25 894.09	[4]
3/2	27 412.44(3)	27 412.36	[4]
5/2	27 715.82(4)	27 715.66	[4]
5/2	34 514.897(30)	34 514.76(5)	[8]

The data of the new levels are listed in table 2. The energy values are given in column 1 (in cm^{-1}), the J-values in column 2, and the hf constants A and B in columns 3 and 4; both are given in MHz. Column 5 shows the wavelength(s) of the excitation line(s) given in Å (in air). When a level involved was found and calculated by considering an unclassified line in the FT spectra using the methods described in [13], its wavelength is bracketed. Column 6 contains additional comments.

The accuracy of the energies of the new levels depends on whether or not the excitation and fluorescence lines appear with a good SNR in the FT spectra, and on the accuracy of the energies of already known levels involved in the transitions. In the very worst case, when no FT wavelengths are available, the wavelength accuracy of our lambda meter (± 0.01 Å) limits the accuracy to ± 0.05 cm^{-1}.

A total of 666 spectral lines could be classified due to our present work, of which 221 lines were excited by laser irradiation and are listed in table 1. The other 445 lines were classified either via laser-induced fluorescence or via their hf pattern and centre of gravity wavenumber, both from the FT spectra. These newly classified lines can be found in tables 5 and 6 of this paper, which are available via Internet only (http://iep.tugraz.at/ta).

An updated complete list of the observed Ta I and Ta II spectral lines as well as a viewing program can be downloaded from the Institute's homepage at http://iep.tugraz.at/ta.

During our investigations we found that the energy values of some previously published levels with even parity did not fit to the experimental results. The corrected energy level values are listed in table 3. The table comprises: in column 1 the angular momenta J; in column 2 the improved energy level values, in column 3 the energy values as previously reported in [4] or [8], which are annotated in column 4.

As an example for the methods used to find a new level, an indepth discussion of the finding of the new level with energy 54 831.88 cm^{-1}, $J = 15/2$, odd parity, follows.

When investigating the FT spectra systematically, we came to a line listed in the spectral tables of MIT [10] with a wavelength $\lambda = 3192.253$ Å and a relative intensity of 70. The line had not been previously classified. In our FT spectra, this spectral line appeared with a centre-of-gravity wavelength of $\lambda = 3192.227$ Å, an hf splitting of about 0.3 Å, and with an SNR of 75 (see figure 1).

In the FT spectra the components of an hf pattern appear with intensity ratios which are very close to the theoretically predicted ratios. A fit of such pattern has to explain not only the position but also the relative intensity of the components.

Table 4. Possible A and B values obtained by fitting the line $\lambda = 3192.227$ Å with different pairs of J values. The quality of the fit indicates the best combination of J values.

Upper level	Lower level	Quality	Upper level		Lower level	
J	J'	of the fit	A (MHz)	B (MHz)	A (MHz)	B (MHz)
8	7	19.3	169(20)	3288(350)	962(2)	1559(2000)
7.5	6.5	19.6	176(10)	2349(650)	995(15)	422(650)
7	6	15.9	177(3)	2329(400)	1053(3)	−73(300)
6.5	5.5	10.7	173(13)	2630(330)	1112(15)	−264(240)
6	5	7.3	177(25)	2292(1000)	1191(30)	−1050(850)

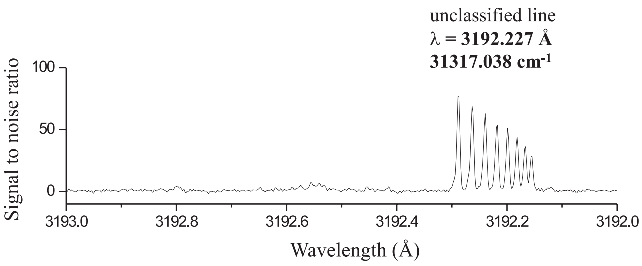

Figure 1. Part of a FT spectrum containing the unclassified Ta line $\lambda = 3192.227$ Å.

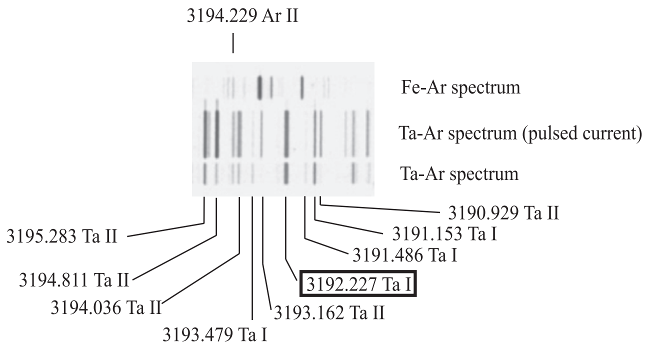

Figure 2. Part of a photoplate containing three spectra. The top Fe–Ar spectrum is used as a reference spectrum. The bottom Ta–Ar spectrum was obtained using a cw hollow cathode lamp. In the middle is a Ta–Ar spectrum obtained using a hollow cathode lamp operated with current pulses. Here Ta II lines appear intensity enhanced. All spectra were produced by a grating spectrograph (focal length 2 m, fifth order).

With eight well-resolved hf components (corresponding to diagonal components of the hf transition, $\Delta F = \Delta J$) and the fact that the smallest component still has a relatively high intensity compared to the highest component (see figure 1), this indicates that levels with high angular momenta are involved in the transition. We tried to fit the line pattern starting with the angular momenta $J = 8$ for the upper level and $J' = 7$ for the lower level, treating the hf constants A and B of both upper and lower levels as free parameters. Then we decreased the J and J' values in steps of 0.5. The hf constants obtained, together with the quality Q of the fit procedure (Q is inversely proportional to the least square error sum) are given in table 4. Almost the same fit quality was obtained for both $J = 8$ to $J' = 7$ and $J = 7.5$ to $J' = 6.5$ combinations. Integer J values correspond to the spectrum of single ionized Ta (Ta II). However, our list of known ionic levels gives no levels with $J > 6$. Thus a transition $J = 8$ to $J' = 7$ is very unlikely.

The assumption that the investigated spectral line is a line belonging to the spectrum of the tantalum atom (Ta I) is confirmed by its appearance in a spectrum on a photographic plate produced during the present work using the grating spectrograph in Poznan (see figure 2). This plate was produced in order to distinguish between lines belonging to the Ta I and the Ta II spectrum. It contains a Fe–Ar spectrum as reference and a Ta–Ar spectrum, both produced by hollow cathode lamps which were operated with a direct current of 100 and 70 mA, respectively. A third Ta–Ar spectrum was produced by a hollow cathode lamp operated with current pulses (50 pulses s, pulse duration ≈1 ms, pulse current ≈100 A). The exposure time of the photoplate was the same for both Ta spectra (cw and pulsed). By comparing both Ta–Ar spectra, one can see, that in the spectrum of the pulsed light source Ta II lines appear much stronger than in the dc discharge, while the intensities of the atomic lines remain constant or become even weaker. The line $\lambda = 3192.227$ Å has the same intensity in both spectra, which supports classifying the line as belonging to the atomic spectrum.

We thus assumed that the investigated line can be explained as the transition from a new level with $J = 7.5$ to a level with $J' = 6.5$. Comparing the fit result of $A = 995$ MHz for the lower level to the A values of known levels with $J' = 6.5$, we found two levels which could serve as lower levels for the transition under investigation: 23 514.923 cm^{-1}, even parity, $A = 965.1(21)$ MHz, $B = 1719(49)$ MHz, and 27 777.9 cm^{-1}, odd parity, $A = 1020.4(21)$ MHz, $B = 1431(49)$ MHz.

Moreover, all other levels with $J' = 6.5$ would lead to an energy of the new upper level above the ionization limit (60 891.4 cm^{-1} [17]).[6] Thus we used the A and B values of the above given levels and fitted the line again, now only treating A and B of the upper level as free parameters. A higher quality fit was obtained with the A and B factors of level 23 514.923 cm^{-1}. The hf constants for the new upper level, $A = 150.3(10)$ MHz and $B = 3658(25)$ MHz, could be obtained with fit quality of 19.0 (see figure 3). Then we added the vacuum wavenumber of the centre-of-gravity wavelength ($\lambda = 3192.227$ Å) to the energy of the lower level and introduced a new upper level 54 831.96 cm^{-1}, $J = 7.5$, odd parity.

Normally, if we introduce a new level, this level should explain the wavenumber and the hf pattern of other, previously unclassified lines. If one of the calculated transitions to known levels is inside the wavelength regions of our lasers, we try to confirm its existence by further excitations. But due to the large angular momentum $J = 15/2$, between 2000 and

[6] References [18–20] are used in tables 5 and 6, which are available via Internet (http://iep.tugraz.at/ta).

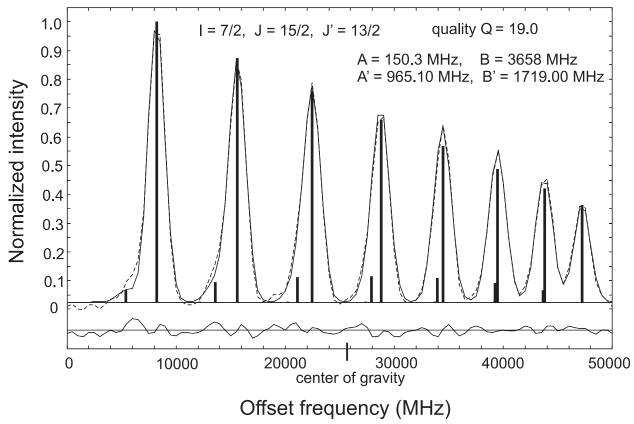

Figure 3. Best fit of the FT spectrum of the line $\lambda = 3192.227$ Å, assuming a transition $J = 15/2$ to $J' = 13/2$. The hf constants A' and B' of the lower level were fixed; the fit procedure used normalized theoretical intensities of the components. The fit procedure treated A, B, and the centre of gravity frequency as free parameters. The lower trace shows the difference between the experimental and the fitted curve.

50 000 Å only three possible transitions to lower $J' = 13/2$ or 15/2 levels are predicted. Of these predicted lines, only $\lambda = 3192.227$ Å appears in the FT spectra. The line $\lambda = 4115.825$ Å does not appear in the FT spectra and is just outside the region of our dye laser working in the blue region.

$\lambda = 46\,740.45$ Å is far in the infrared region and also does not appear in the FT spectra. Nevertheless, we believe that introduction of this level is correct.

Table 5 and 6, which contain lines classified via laser-induced fluorescence and via the hf patterns observed in the FT spectra, are available only via Internet. These tables are similar to tables 2 and 3 in [9].

4. Conclusion

In recent years, we have been able to clearly classify a large number of additional lines obtained from our FT spectra. In some cases, previously unknown energy levels were found, enlarging the knowledge of the fine structure of the Ta I level scheme using the hf structure of the spectral lines. The presented work demonstrates again how successful laser spectroscopic investigations of spectral lines supplemented by the evaluation of high-resolution FT spectra is, combined with spectra of different light sources. Future projects focus on improving knowledge about Ta I and Ta II lines in the ultraviolet region.

Acknowledgment

The presented work has been supported by Austrian Science Fund, project no. P 15425.

References

[1] Guthöhrlein G H and Windholz L 1993 *Z. Phys.* D **27** 343
[2] Hammerl H, Guthöhrlein G H, Elantkovska M, Funtov V, Gwehenberger G and Windholz L 1995 *Z. Phys.* D **33** 97
[3] Mocnik H, Arcimowicz B, Salmhofer W, Windholz L and Guthöhrlein G H 1996 *Z. Phys.* D **36** 129
[4] Messnarz D and Guthöhrlein G H 2000 *Eur. Phys. J.* D **12** 269
[5] Arcimowicz B, Huss A, Roth S, Jaritz N, Messnarz D, Guthöhrlein G H, Jäger H and Windholz L 2001 *Eur. Phys. J.* D **13** 187
[6] Jaritz N, Jäger H and Windholz L 2002 *Eur. Phys. J.* D **18** 267
[7] Messnarz D, Jaritz N, Arcimowicz B, Zilio V O, Engleman R J, Pickering J C, Jäger H, Guthöhrlein G H and Windholz L 2003 *Phys. Scr.* **68** 170
[8] Jaritz N, Guthöhrlein G H, Windholz L, Messnarz D, Engleman R J, Pickering J C and Jäger H 2004 *Phys. Scr.* **69** 441
[9] Jaritz N, Windholz L, Messnarz D, Jäger H and Engleman R J 2005 *Phys. Scr.* **71** 611
[10] Harrison G R 1985 *Massachusetts Institute of Technology Wavelength Tables* 4th edn (Cambridge, MA: MIT Press)
[11] Meggers W F, Corliss C H and Scribner B F 1975 *Natl. Bur. Stand. (US)* Monograph 145-Part I
[12] Meggers W F, Corliss C H and Scribner B F 1961 *Natl. Bur. Stand. (US)* Monograph 32-Part I
[13] Windholz L and Guthöhrlein G H 2003 *Phys. Scr.* T **105** 55
[14] Peck E R and Reeder K 1972 *J. Opt. Soc. Am.* **62** 958
[15] Pickering J C 1996 *Astrophys. J. Suppl.* **107** 811
[16] Engleman R Jr 1987 Improved analyses of Ta I and Ta II *Symposium on Atomic Spectroscopy and Highly-Ionized Atoms, Lisle, IL (16 August 1987)* Engleman R Jr *et al* in preparation
[17] Simard B, Kowalczyk P and James A M 1994 *Phys. Rev.* A **50** 846
[18] Van den Berg G J, Klinkenberg P F A and Van den Bosch J C 1952 *Physica* **18** 221
[19] Kiess C C 1962 *J. Res. Natl. Bur. Std.* A **66** 111
[20] Klinkenberg P F A, Van den Berg G J and Van den Bosch J C 1950 *Physica* **16** 861